SR POWER DISTRIBUTION ALONG WIGGLER SECTION OF ILC DR*

K. Zolotarev, BINP, Novosibirsk, Russia
O.B. Malyshev†, ASTeC, STFC DL and Cockcroft Institute, Warrington, UK
M. Korostelev, A. Wolski, Department of Physics, University of Liverpool, Liverpool, and Cockcroft Institute, Warrington, UK.
J.M. Lucas, N. Collomb, S. Postlethwaite, ETC, STFC DL and Cockcroft Institute, Warrington, UK

Abstract

A long wiggler section is required in each ILC damping ring to provide short radiation damping times. Synchrotron radiation (SR) generated by the beam in the wigglers must be absorbed by different components of the vacuum vessel, including specially designed absorbers. The optimisation of the mechanical design, vacuum system and electron cloud mitigation requires accurate calculation of the SR power distribution. The angular power distribution from a single wiggler was calculated (with software developed in-house) based on the latest lattice design [1]. Then the superposition of SR from all wigglers allows calculation of the power distribution for all components along the wiggler section and the downstream straight section.

INTRODUCTION

The ILC positron damping ring (DR) in the DCO4 lattice design [1] contains a 374 m long wiggler section, consisting of 88 consecutive wiggler modules. The design of this section is driven by a number of different requirements, including beam dynamics, aperture, electron cloud mitigation, vacuum specification, SR power absorption and cost [2]. Nominally, the electron damping ring uses the same length of wiggler, although this could be reduced, because the beam from the electron source is smaller than that from the positron source, and therefore requires less damping.

One of the requirements from electron cloud mitigation is that the photon flux on the vacuum chamber inside wigglers and quadrupoles must be kept to a minimum. The BPMs required in each module should also be screened from SR to reduce background noise. This means that a lumped SR absorber is required at the exit of each wiggler module. Design of the system for power absorption is made challenging by the fact that the SR power from the wiggler is emitted in a narrow angle, and the power density reaches values sufficient to destroy the material of the vacuum chamber. To optimise the engineering solution, the SR power density distribution on different parts of the vacuum chamber must be calculated. Generally, some iteration is required between the mechanical design and the calculation of the SR power density distribution, before the design is finalised.

In this paper, we report the main steps and results of the design optimization procedure for the ILC DR wiggler section.

CALULATION OF SR POWER DISTRIBUTION

The angular distribution of SR power density can be estimated with a formula obtained by integrating the power density spectrum [3]:

$$\frac{dP}{d\Omega} = \frac{d^2P}{d\theta\, d\psi} = P_T \frac{21\gamma^2}{16\pi K} f_x\left(\frac{\gamma\theta}{K}\right) f_z(\gamma\psi), \qquad (1)$$

Where $P_T(kW) = 0.633\, E^2(GeV)\, B_w^2(T)\, L(m)\, I(A)$ is the full power of SR emitted by a wiggler, E is the beam energy, B_w is the peak field in the wiggler, L is the wiggler length and I is the beam current. The functions f_x and f_z describe the horizontal and vertical distribution of the power density and can be written as:

$$f_x(a) = \begin{cases} \frac{2}{\pi}\sqrt{1-a^2} & \text{for } a < 1, \\ 0 & \text{for } a \geq 1; \end{cases} \qquad (2)$$

$$f_z(b) = \frac{21}{32}\left[\frac{1}{(1+b^2)^{5/2}} + \frac{5b^2}{7(1+b^2)^{7/2}}\right].$$

A similar approach was used previously in the design of the vacuum chamber and the calculation of SR power absorption for PETRA-III [4]. After the successful commissioning of PETRA-III, the calculated and experimentally measured values for the absorbed power were found to be in very good agreement.

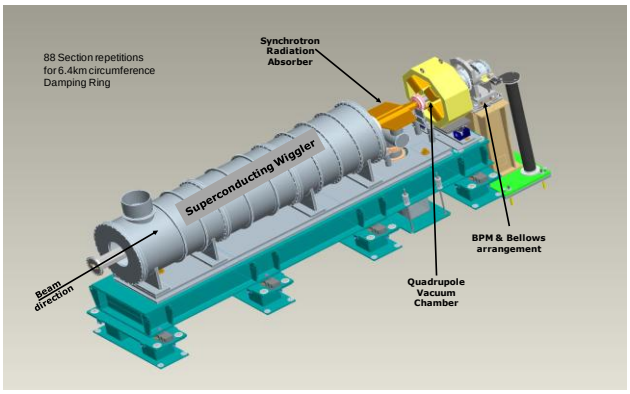

Figure 1: Layout of the ILC DR wiggler module.

* Work supported by the Science and Technology Facilities Council, UK.
† oleg.malyshev@stfc.ac.uk

MECHANICAL DESIGN

The mechanical and vacuum design of the wiggler section vacuum chamber is described in detail in Ref. [2]. One ILC DR wiggler module (shown in Fig. 1) consists of a superconducting wiggler, SR power absorber, quadrupole magnet, and BPM. Each of these components has its own vacuum chamber. The 2995 mm long wiggler vacuum chamber (see the cross section shown in Fig. 2) has a circular beam chamber, and two ante-chambers.

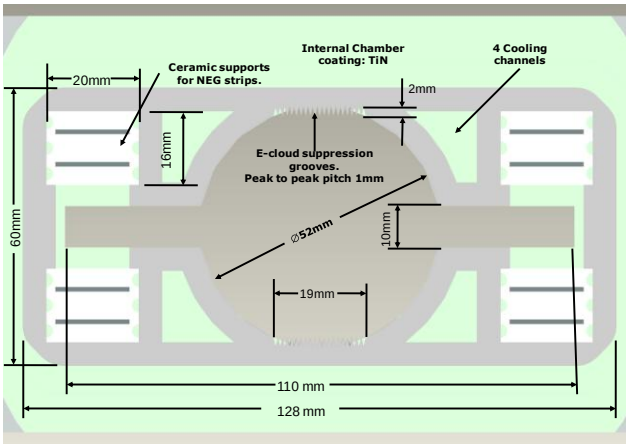

Figure 2: Cross section of wiggler vacuum chamber.

The 499 mm long SR absorber shown in Fig. 3 should absorb ideally all, or at least the greater part, of the SR power. The angled surfaces in the ante-chamber of the absorber will intercept all SR that passes through the wiggler ante-chamber. The beampipe aperture tapers smoothly from internal diameter 52 mm to 44 mm, and then back to 52 mm. This creates a shadow for the following quadrupole and BMP vacuum chambers, which were modelled as simple circular tubes with internal diameter of 52 mm.

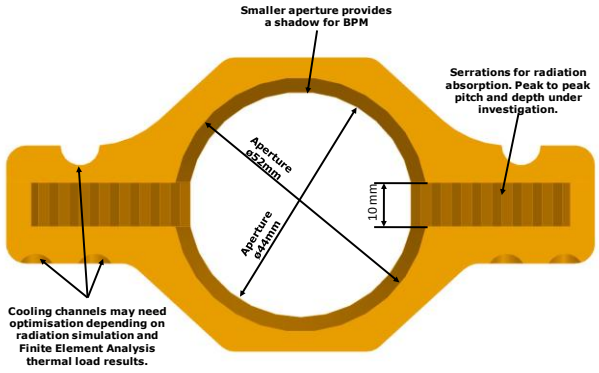

Figure 3: SR power absorber

The impedance of the chamber in the wiggler section has been modelled, and found to be small compared to the total impedance of the BPMs [5]. Tracking simulations show that the combined impedance from the wiggler section and the BPMs allows a considerable margin between nominal operating conditions and the instability threshold.

SR POWER DISTRIBUTION

Actual parameters used for the calculations of SR power distribution in the ILC DR wiggler section are presented in Table 1. Since the inner surface of the vacuum chamber has a complicated shape with some elements creating a shadow on others, an angular sweep of the internal view of the wiggler section components of vacuum chamber has been constructed from the centre of the first wiggler. A quarter of the scan is shown in Fig. 4. In this view visible elements of the chamber are represented as flat contours. The invisible parts are excluded by the properties of the contour plot.

Table 1: Main beam and wiggler parameters.

Parameter	Symbol	Value
Field amplitude	$B\,[T]$	1.6
Electron energy	$E\,[GeV]$	5
Maximal beam current	$I\,[mA]$	400
Relativistic factor	$\gamma = E/(mc^2)$	9785
Wiggler period	$\lambda_w\,[m]$	0.4
SR critical energy	$\varepsilon_c[keV] = 0.655E^2[GeV]B[T]$	36.78
K-parameter	$K = 0.934\lambda_w\,[cm]\,B\,[T]$	59.776
Wiggler length	$L\,[m]$	2.45
Wiggler SR power	$P_T[kW] = 0.633\,I[A]\times$ $\times E^2[GeV]B^2[T]L[m]$	39.702
Vertical SR spread	$\theta_v\,[\mu rad] = \gamma^{-1}$	102.2
Horizontal SR spread	$\theta_h\,[\mu rad] = 2K/\gamma$	12.22

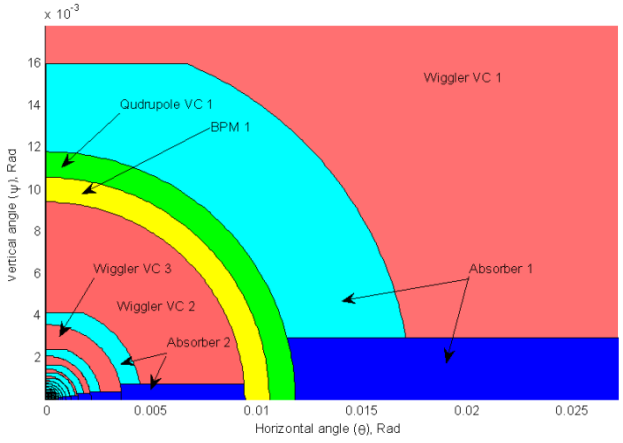

Figure 4: Angular visibility of wiggler section components from centre of 1st wiggler.

The power falling on individual elements was then calculated by integrating formula (1) over flat areas covered by the contours of elements. For numerical

implementation of the integration, the area integration is reduced to integration over the boundary contour, based on Stokes' theorem:

$$\oint_L \mathbf{A} \cdot d\mathbf{l} = \int_S \mathbf{rot}\,\mathbf{A}\, d\mathbf{s} \qquad (3)$$

In this case, because of the reduction in the number of dimensions, the choice of integration step and the convergence analysis becomes easier. The results of the integration are presented in Fig. 5.

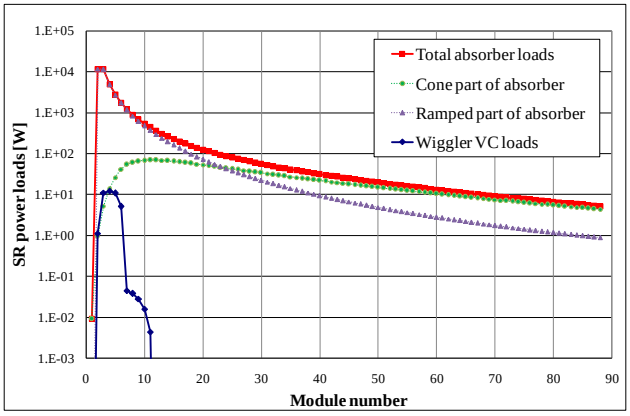

Figure 5: Power dissipation from 1st wiggler along the wiggler section.

It is obvious that the total load on each element is composed of individual loads from all upstream wigglers. Therefore, the total load on each element was calculated by summing the appropriate values; the results are listed in Table 2, and shown in Fig. 6.

Table 2. Power dissipation [W] along the wiggler section.

Module number	Wiggler vac. ch.	Absorber		
		ramped	cone	total
1	0	0	0.01	0.01
2	1.1	11731	1.0	11732
3	12.1	23216	6.2	23222
4	24.4	28076	20	28096
5	35.1	30785	45	30830
6	40.2	32493	87	32580
10	40.3	35580	335	35915
20	40.3	37344	958	38302
40	40.3	37870	1638	39508
88	40.3	38015	2126	40141

The first wiggler vacuum chamber is not irradiated; but then the SR power steadily increases to the level of about 40 watts in the sixth wiggler vacuum chamber. The power load on the vacuum chambers in subsequent wigglers remains roughly constant. The absorbers take most of the power; however, the power load on the first absorber is negligible, therefore it could be replaced with a simple tube with a pumping port. The power dissipation in the following absorber is already above 10 kW and steadily grows to 30 kW in the fifth absorber, then slowly increases with module number reaching the highest power load of about 40.2 kW in the last absorber. Quadrupole and BPM vacuum chambers are well protected from SR, receiving less than 9 mW each. It is important to mention here that photon reflectivity was not included in these calculations.

It is also important to know the SR power passing through all modules and continuing downstream to the fist arc dipole. The total power of 256 kW not absorbed within the wiggler section should be absorbed with a special high power absorber.

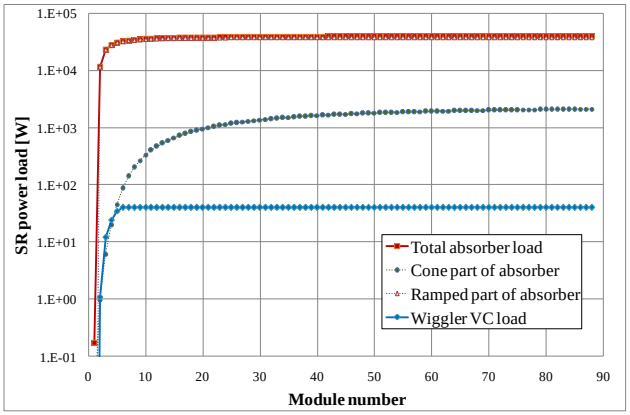

Figure 6: Power dissipation in wiggler vacuum chamber and SR power absorbers along the wiggler section.

CONCLUSIONS

A power dissipation model for the ILC damping ring wiggler section has been constructed. The results show that the wiggler, quadrupole and BPM vacuum chamber can be efficiently screened with an SR power absorber. The system design meets the main engineering and beam dynamics criteria. The absorber design should be capable of absorbing up to 40.2 kW of SR power. SR flux with the power of 256 kW following the wiggler section should be absorbed with a special high power absorber near first arc dipole.

REFERENCES

[1] M. Korostelev *et al*, "DCO4 lattice design for 6.4 km ILC damping ring", these proceedings (IPAC'10).

[2] O.B. Malyshev, J.M. Lucas, N. Collomb *et al*, "Mechanical and vacuum design of wiggler section of ILC DR", these proceedings.

[3] K.-J. Kim, "Angular distribution of undulator power for an arbitrary deflection parameter K", Nucl. Instrum. and Meth. in Phys. Res. A246 (1986), p. 67.

[4] K. Balewski, "Comissioning of PETRA III", these proceedings.

[5] M. Korostelev and A. Wolski, "Impedance and single-bunch instabilities in the ILC damping ring", these proceedings.